RESEARCH PAPER

Development and Optimization of Rutin-Loaded Intranasal Nanoemulsion for Enhanced Nasal Permeation and Drug Release

Preetha Puthezhath[1*], C. K. Dhanapal[2], B. Dinesh Kumar[3]

[1]Annamalai University PhD Scholar and St James College of Pharmaceutical Sciences, Kerala, India

[2]Annamalai University, Tamil Nadu, India

[3]St James College of Pharmaceutical Sciences, Kerala, India

Corresponding author:

Email: angelpreetha@rediffmail.com

ABSTRACT

The effective treatment of central nervous system (CNS) disorders remains a major challenge due to the restrictive nature of the blood–brain barrier (BBB), which limits the delivery of therapeutic agents to the brain. Intranasal drug delivery has emerged as a promising non-invasive approach for direct nose-to-brain transport, bypassing the BBB and improving brain bioavailability. The present study aimed to develop and optimize a rutin-loaded intranasal nanoemulsion for enhanced nasal permeation and drug release using a low-pressure homogenization technique. Rutin, a naturally occurring flavonoid with potent antioxidant and neuroprotective properties, suffers from poor aqueous solubility and low oral bioavailability, thereby limiting its therapeutic application in neurological disorders.

Nanoemulsions were formulated using oleic acid as the oil phase, Cremophor EL as surfactant, and polyethylene glycol 400 as co-surfactant. Pseudo ternary phase diagrams were constructed to identify the nanoemulsion region, and formulations were optimized based on droplet size, zeta potential, and drug release characteristics. The optimized formulation exhibited a droplet size of approximately 76 nm with narrow size distribution and satisfactory zeta potential, indicating good physical stability. In vitro drug release studies demonstrated sustained and enhanced release of rutin from the nanoemulsion compared to conventional formulations. Ex vivo nasal permeation studies further revealed improved permeation across nasal mucosa, suggesting enhanced nose-to-brain delivery potential.

The developed nanoemulsion showed acceptable physicochemical characteristics, stability, isotonicity, and compatibility for intranasal administration. The findings suggest that intranasal nanoemulsion-based delivery of rutin may represent a promising strategy for improving brain targeting and therapeutic efficacy of neuroprotective agents. Furthermore, the study highlights the potential of low-pressure homogenization as a simple, cost-effective, and scalable approach for the development of intranasal nanoemulsion systems for CNS drug delivery.

Keywords: Rutin; Intranasal delivery; Nanoemulsion; Nose-to-brain delivery; Blood–brain barrier; Neuroprotection; Low-energy homogenization; Nasal permeation.

How to cite this article: Puthezhath P, Dhanapal CK, Dinesh Kumar B. Development and Optimization of Rutin-Loaded Intranasal Nanoemulsion for Enhanced Nasal Permeation and Drug Release. Int J Drug Deliv Technol. 2026;16(53s): 333-357. DOI: 10.25258/ijddt.16.53s.81

Source of support: Nil.

Conflict of interest: None.

1. Introduction

1.1 Neurological Disorders and Challenges in Brain Drug Delivery

Neurological disorders are among the leading causes of disability and mortality worldwide and represent a major public health challenge. Disorders such as Alzheimer's disease, Parkinson's disease, epilepsy, cerebral ischemia, multiple sclerosis, dementia, and other neurodegenerative diseases are characterized by progressive neuronal degeneration, oxidative stress, inflammation, mitochondrial dysfunction, and neurotransmitter imbalance [1,2]. These pathological alterations significantly impair cognitive and motor functions and adversely affect the quality of life of patients.

Despite considerable advancements in neuroscience and pharmaceutical research, effective treatment of central nervous system (CNS) disorders remains difficult because of the complex structure and physiology of the brain. One of the major obstacles in CNS drug delivery is the presence of the blood–brain barrier (BBB), which restricts the transport of most therapeutic agents into the brain tissue [3]. The BBB is a highly specialized physiological barrier composed of tightly connected endothelial cells, astrocytes, pericytes, basement membrane, and associated neuronal cells, collectively referred to as the neurovascular unit [4].

The BBB serves a protective role by maintaining brain homeostasis and preventing the entry of toxins,

pathogens, and harmful substances from systemic circulation into the CNS. However, the same protective mechanism also limits the penetration of hydrophilic drugs, peptides, proteins, and many neuroprotective agents [5]. It has been reported that approximately 98% of small-molecule drugs and nearly all macromolecular therapeutics fail to cross the BBB in therapeutically effective concentrations [6].

The BBB contains tight junction proteins such as occludin, claudins, and zonula occludens proteins that restrict paracellular transport of molecules [7]. In addition, the presence of efflux transporters, metabolic enzymes, and selective transport systems further reduces drug permeability across the barrier [8]. Consequently, conventional routes of drug administration, including oral and parenteral delivery, often fail to achieve adequate drug concentrations in the brain.

Oral administration of drugs intended for CNS delivery is associated with poor bioavailability due to gastrointestinal degradation, hepatic first-pass metabolism, and limited BBB permeability [9]. Similarly, intravenous administration may require high systemic doses to achieve therapeutic drug concentrations in the brain, leading to systemic toxicity and adverse effects [10]. Therefore, there is a growing need for alternative and efficient drug delivery approaches capable of bypassing the BBB and improving brain targeting.

Several strategies have been investigated to overcome BBB-associated limitations, including osmotic BBB disruption, prodrug approaches, receptor-mediated transport, carrier-mediated transport, and nanotechnology-based delivery systems [11]. Among these approaches, non-invasive drug delivery systems have gained increasing attention because of their improved patient compliance and reduced systemic toxicity.

1.2 Intranasal Drug Delivery for Brain Targeting

Intranasal drug delivery has emerged as a promising non-invasive approach for direct nose-to-brain transport. The nasal cavity possesses unique anatomical and physiological connections with the CNS through the olfactory and trigeminal nerve pathways, enabling drugs to bypass the BBB and directly access the brain [12].

The olfactory region, located in the upper posterior portion of the nasal cavity, provides direct communication between the nasal mucosa and the olfactory bulb of the brain. Drugs administered intranasally can be transported through olfactory neurons into the CNS via intracellular and extracellular pathways [13]. In addition, the trigeminal nerve pathway enables transport of therapeutic agents from the respiratory epithelium to deeper brain regions and the brainstem [14].

Intranasal administration offers several advantages over conventional routes of delivery. These include rapid onset of action, avoidance of hepatic first-pass metabolism, reduced systemic exposure, non-invasive administration, and improved patient compliance [15]. Furthermore, intranasal delivery can improve brain bioavailability of drugs that exhibit poor permeability across the BBB.

Despite these advantages, intranasal drug delivery faces several physiological challenges. The nasal cavity possesses defense mechanisms such as mucociliary clearance, enzymatic degradation, and limited residence time, which may reduce drug absorption [16]. In addition, the permeability of hydrophilic and poorly soluble drugs across the nasal epithelium is limited. Therefore, advanced formulation strategies are required to improve nasal retention, drug permeation, and formulation stability.

Permeation enhancers, mucoadhesive agents, and nanocarrier systems have been investigated to improve intranasal drug delivery efficiency [17]. Among these approaches, nanoemulsion-based systems have shown significant promise due to their ability to improve solubilization and permeation of poorly water-soluble drugs.

1.3 Nanoemulsions as Advanced Drug Delivery Systems

Nanoemulsions are kinetically stable colloidal dispersions composed of oil, water, surfactant, and co-surfactant, with droplet sizes generally ranging between 20 and 200 nm [18]. Due to their nanoscale droplet size and large interfacial surface area, nanoemulsions enhance drug solubilization, dissolution rate, membrane permeability, and bioavailability [19].

Nanoemulsions have gained considerable interest for CNS drug delivery because of their ability to improve transport across biological membranes and facilitate brain targeting [20]. The small droplet size allows intimate contact with the nasal mucosa and promotes enhanced absorption through transcellular and paracellular pathways [21].

For intranasal applications, nanoemulsions offer several additional advantages, including improved mucoadhesion, prolonged nasal residence time, protection against enzymatic degradation, and enhanced permeation through epithelial barriers [22]. Surfactants and co-surfactants present in nanoemulsions may alter membrane fluidity and

transiently open tight junctions, thereby facilitating drug transport across the nasal epithelium [23].

Nanoemulsion formulations have been investigated for the delivery of several CNS-active drugs, including antiepileptics, antidepressants, antipsychotics, and neuroprotective agents [24]. These studies have demonstrated improved nose-to-brain transport and enhanced therapeutic efficacy compared to conventional dosage forms.

The physicochemical characteristics and performance of nanoemulsions are highly dependent on formulation variables such as oil phase selection, surfactant concentration, co-surfactant ratio, and method of preparation [25]. Therefore, optimization of these variables is essential to achieve desirable droplet size, stability, zeta potential, and drug release characteristics.

1.4 Methods of Nanoemulsion Preparation

Nanoemulsions can be prepared using high-energy and low-energy techniques. High-energy methods include ultrasonication and high-pressure homogenization, which employ intense mechanical forces to reduce droplet size [26]. Although these methods are effective, they may involve high operational costs, excessive energy consumption, and possible degradation of thermolabile compounds.

Low-energy techniques such as spontaneous emulsification, phase inversion temperature method, and low-pressure homogenization have gained attention because of their simplicity, scalability, and suitability for heat-sensitive compounds [27].

Low-pressure homogenization is a cost-effective and scalable technique that produces nano-sized droplets under relatively low shear stress and minimal thermal exposure [28]. This method is particularly suitable for phytoconstituents and natural compounds whose biological activity may be affected by excessive heat or mechanical stress. Despite its advantages, the use of low-pressure homogenization for intranasal nanoemulsion-based brain delivery remains relatively underexplored.

1.5 Rutin as a Neuroprotective Phytoconstituent

Phytoconstituents with antioxidant and neuroprotective activities have gained increasing importance in the management of neurodegenerative disorders. Among these compounds, rutin has attracted considerable attention because of its broad spectrum of pharmacological activities [29].

Rutin is a naturally occurring flavonoid glycoside composed of quercetin and rutinose. It is widely distributed in fruits, vegetables, tea, and medicinal plants [30]. Rutin exhibits antioxidant, anti-inflammatory, anti-apoptotic, vasoprotective, cardioprotective, and neuroprotective activities [31].

Several experimental studies have demonstrated that rutin can scavenge free radicals, inhibit lipid peroxidation, suppress inflammatory mediators, and protect neuronal cells against oxidative stress-induced damage [32]. Rutin has shown therapeutic potential in models of Alzheimer's disease, Parkinson's disease, cerebral ischemia, and other neurodegenerative disorders [33].

Despite its promising pharmacological properties, the therapeutic application of rutin is limited because of its poor aqueous solubility, low oral bioavailability, and extensive first-pass metabolism [34]. Conventional oral administration fails to achieve sufficient drug concentration in the brain, thereby limiting its neuroprotective efficacy. Therefore, the development of advanced drug delivery systems capable of enhancing the solubility, stability, and brain bioavailability of rutin is essential.

1.6 Rationale of the Present Study

The integration of intranasal drug delivery with nanoemulsion technology offers a promising strategy to overcome the pharmacokinetic limitations associated with rutin. Intranasal administration facilitates direct nose-to-brain transport while bypassing the BBB, whereas nanoemulsion systems improve drug solubility, permeation, and stability [35]. Low-pressure homogenization further provides advantages such as reduced energy consumption, minimal thermal degradation, formulation simplicity, and scalability. Although various nano formulation approaches have been explored for rutin delivery, limited studies are available on intranasal rutin nanoemulsions prepared using low-pressure homogenization techniques.

Therefore, the present research was undertaken to develop and optimize a rutin-loaded intranasal nanoemulsion using low-pressure homogenization with the objective of enhancing nasal permeation and drug release. The study further aims to evaluate the physicochemical characteristics, stability, and in vitro performance of the developed formulation for potential brain-targeted drug delivery applications.

2. Materials and Methods:

Materials and Methods

2.1 Materials

Rutin hydrate was obtained from a certified pharmaceutical supplier and used as the active pharmaceutical ingredient. Oleic acid was selected as the oil phase owing to its high solubilization capacity for lipophilic flavonoids. Cremophor® EL and Polyethylene glycol 400 (PEG 400) were employed as

surfactant and co-surfactant, respectively. Chitosan was utilized as a mucoadhesive polymer to enhance nasal residence time and permeation. Methanol, ethanol, phosphate-buffered saline (PBS), and other analytical-grade reagents were procured from standard commercial suppliers and used without further purification. Freshly prepared double-distilled water was used throughout the study. [35,36]

2.2 Preformulation

2.2.1 Solubility Studies

The solubility of rutin was determined in various oils, surfactants, and co-surfactants using the shake-flask method. Excess rutin was added separately into vials containing different vehicles, including oleic acid, Cremophor EL, and PEG 400. The mixtures were vortexed and shaken in an orbital shaker at 25 ± 1°C for 72 h to attain equilibrium. The samples were centrifuged at 5000 rpm for 15 min, and the supernatant was filtered through a 0.45 µm membrane filter. The concentration of dissolved rutin was quantified spectrophotometrically at 257 nm after suitable dilution. [37,38]

2.2.2 Drug–Excipient Compatibility Studies

Compatibility between rutin and excipients was assessed using Fourier-transform infrared spectroscopy (FTIR). Spectra of pure rutin, individual excipients, and optimized formulation were recorded over the range of 4000–400 cm^{-1} using the potassium bromide pellet method. The obtained spectra were analyzed for characteristic peaks and possible interactions. [39]

2.2.3 Construction of Pseudoternary Phase Diagram

Pseudoternary phase diagrams were constructed using the water titration method to identify the nanoemulsion region. Surfactant and co-surfactant mixtures (Smix) were prepared in different ratios (2:1, 3:1, and 4:1). The oil phase and Smix were mixed in varying proportions, followed by gradual titration with distilled water under continuous magnetic stirring. The transparency and flowability of formulations were visually observed to determine the nanoemulsion region. The obtained data were plotted using suitable software to generate phase diagrams. [40,41]

2.2.4 Optimization of Nanoemulsion by Design of Experiments

A three-factor, three-level Box–Behnken design was employed for optimization of the nanoemulsion formulation using Design-Expert® software. Independent variables included oil concentration (A), Smix ratio (B), and total Smix concentration (C), whereas dependent variables were particle size, zeta potential, and cumulative drug release. Experimental runs were generated by the software, and statistical analysis was performed to identify the optimized formulation. Response surface plots and polynomial equations were generated to evaluate the effect of formulation variables. [44]

2.3 Formulation of Rutin Intranasal Nanoemulsion

Rutin-loaded nanoemulsion formulations were prepared by using low energy homogenization (magnetic stirring) followed by ultrasonication. The oil phase and aqueous phase were mixed and homogenized at 1000rpm for 2 hours with intermittent stirring at 30min interval to obtain a coarse emulsion. The resultant emulsion was further subjected to ultrasonication for nano size reduction and formation of rutin nanoemulsion [42,43]

2.4 Characterization of Nanoemulsion

2.4.1 Particle Size, Polydispersity Index, and Zeta Potential

The mean droplet size, polydispersity index (PDI), and zeta potential of the prepared nanoemulsion were determined using dynamic light scattering (DLS) with a Zetasizer instrument. Samples were diluted appropriately with distilled water before analysis to avoid multiple scattering effects. Measurements were performed in triplicate at 25°C. [45,46]

2.4.2 pH, Viscosity, Percentage transmittance, Refractive index, Conductivity and Osmolarity Determination

The pH of the optimized formulation was measured using a calibrated digital pH meter at room temperature to ensure compatibility with the nasal mucosa. Measurements were performed in triplicate.

The viscosity of the nanoemulsion was determined using a Brookfield viscometer at 25 ± 1°C using an appropriate spindle at predetermined rotational speed.

The transparency of rutin nanoemulsion is determined by measuring the percentage of light transmitted through the formulation using uv visible spectrophotometer. The percentage transmittance value is calculated at 650nm using uv visible spectrophotometer [47,48].

Refractive index measures the extent to which light bends when passing through the nanoemulsion and helps assess its isotropic nature. A few drops of nanoemulsion is placed on the prism surface of refractometer which is calibrated using distilled water and refractive index is measured at room temperature. A refractive index close to that of continuous phase indicates uniformity and transparency of nanoemulsion.

Conductivity measures the ability of the nanoemulsion to conduct electric current and helps to identify the

type of emulsion system. The conductivity probe is immersed completely in the sample and record the conductivity value. Higher conductivity generally indicates oil in water nanoemulsion while very low conductivity suggests water in oil emulsion.

Osmolarity indicates the total concentration of osmotically active particles in the formulation and is particularly important for intranasal formulations to ensure physiological compatibility. The required volume of nanoemulsion is placed into sample holder of osmometer and osmolarity is measured in mOsmol/L [55,56].

2.4.3 Drug Content Determination

An accurately measured quantity of nanoemulsion equivalent to a known amount of rutin was diluted with methanol and analyzed spectrophotometrically at 257 nm after suitable dilution. Drug content was calculated using a previously prepared calibration curve. [49]

2.4.4 Sterility Testing

Sterility testing of the optimized formulation was performed according to pharmacopeial guidelines using fluid thioglycollate medium and soybean casein digest medium. Samples were incubated at appropriate temperatures for 14 days and observed for microbial growth. [54]

2.5 In Vitro Drug Release Study

The in vitro drug release study was performed using a dialysis membrane diffusion method. The dialysis membrane was mounted between donor and receptor compartments containing phosphate-buffered saline (pH 6.4) maintained at 37 ± 0.5°C under continuous stirring. Samples were withdrawn at predetermined intervals and replaced with fresh medium. The amount of rutin released was analyzed spectrophotometrically at 257 nm. [51]

2.6 Mucoadhesive Strength Study

The mucoadhesive strength of the chitosan-containing nanoemulsion was evaluated using a modified physical balance method employing excised goat nasal mucosa. The force required to detach the formulation from the mucosal surface was recorded as the mucoadhesive strength. [53]

2.7 Ex Vivo Nasal Permeation Study

Ex vivo permeation studies were carried out using freshly excised goat nasal mucosa mounted on a Franz diffusion cell. The receptor compartment was filled with phosphate-buffered saline (pH 6.4) maintained at 37 ± 0.5°C. Samples were collected at predetermined intervals and analyzed for rutin content using UV-visible spectrophotometry. Flux and permeability coefficient were calculated to evaluate permeation characteristics. [52]

2.8 Thermodynamic Stability Studies

Thermodynamic stability studies were carried out to evaluate the physical stability of the prepared nanoemulsion. The formulations were subjected to centrifugation at 5000 rpm for 30 min, heating–cooling cycles between 4°C and 45°C, and freeze–thaw cycles between −20°C and 25°C. Formulations showing no phase separation, creaming, or cracking were considered stable. [50]

2.9 Storage Stability Studies

Storage stability studies were performed according to the guidelines of the International Council for Harmonization (ICH) to evaluate the physical and chemical stability of the optimized rutin intranasal nanoemulsion. The formulation was stored under different storage conditions, including refrigerated condition (4 ± 2°C), room temperature (25 ± 2°C), and accelerated condition (40 ± 2°C/75% RH). Samples were withdrawn at predetermined intervals of 0, 1, 2, and 3 months for evaluation. [57]

At each sampling interval, the formulation was assessed for mean droplet size, polydispersity index (PDI), zeta potential, pH, drug content (% remaining), and visual appearance. Droplet size, PDI, and zeta potential were determined using dynamic light scattering techniques, while pH was measured using a calibrated digital pH meter. Drug content was estimated spectrophotometrically after suitable dilution. Visual inspection was carried out to detect any signs of phase separation, creaming, precipitation, or changes in appearance. [58,59]

The nanoemulsion was considered stable when no phase separation or creaming was observed, minimal changes in droplet size and PDI occurred, drug content remained within acceptable limits (90–110%), and pH remained relatively constant throughout the study period. [60]

3. Results and Discussion:

3.1 Preformulation Studies

3.1.1 Solubility Studies

Rutin showed highest solubility in oleic acid among the tested oils, which justified its selection as the oil phase. Surfactant Cremophor EL and co-surfactant PEG 400 demonstrated excellent solubilizing capacity for rutin, facilitating the formation of a stable nanoemulsion. The solubility data are consistent with literature reports indicating oleic acid's suitability for lipophilic drug delivery and Cremophor EL's biocompatibility in nasal formulations.

Table 1: Solubility of Rutin Hydrate in Various Vehicles

S No	Vehicle	Solubility (mg/ml)

1	Cremophor	1.22
2	PEG 400	0.855
3	Tween 80	1.12
4	Propylene glycol	0.736
5	Isopropyl myristate	0.011
6	Oleic acid	0.205
7	Alcohol	0.984

The selection of formulation components was primarily based on the solubility profile of rutin hydrate in various vehicles, along with their physicochemical properties, safety, and suitability for pharmaceutical use.

Cremophor was selected as the surfactant due to its highest solubilizing capacity for rutin hydrate among the tested vehicles (1.22 mg/mL). Cremophor is a non-ionic surfactant with a high hydrophilic–lipophilic balance (HLB), which promotes efficient micelle formation and drug encapsulation. Its ability to significantly enhance solubility makes it suitable for improving the dissolution and bioavailability of poorly water-soluble drugs such as rutin hydrate. Additionally, Cremophor is widely used in oral and topical formulations owing to its acceptable safety profile and compatibility with other formulation components.

PEG 400 was chosen as the co-surfactant based on its comparatively high solubility of rutin hydrate (0.855 mg/mL). PEG 400 acts as a co-solubilizer, reducing interfacial tension and increasing the flexibility of the interfacial film, which is critical for the spontaneous formation of stable emulsified systems. The presence of PEG 400 enhances the dispersibility of the surfactant in the oil phase and supports the formation of fine droplets, thereby improving drug loading and formulation stability. Moreover, PEG 400 is pharmaceutically accepted and exhibits good miscibility with Cremophor.

Fig 1: FTIR overlay of Rutin with excipients

Oleic acid was selected as the oil phase as it demonstrated better solubilization capacity (0.205 mg/mL) compared to other oily vehicles such as isopropyl myristate. Oleic acid is a long-chain fatty acid known for its excellent drug-solubilizing properties and ability to act as a permeation enhancer, which can further improve the absorption of rutin hydrate. Its compatibility with non-ionic surfactants and its widespread use in pharmaceutical formulations justify its selection as a suitable oil phase.

The combination of Cremophor, PEG 400, and oleic acid is expected to form a thermodynamically stable system capable of enhancing the solubility and bioavailability of rutin hydrate. The selected components exhibit high mutual compatibility, effective solubilization, and regulatory acceptability, making them suitable for the development of advanced drug delivery systems such as nanoemulsions.

3.1.2 Drug–Excipient Compatibility

FTIR spectra of rutin, excipients, and their physical mixtures showed no significant changes in characteristic peaks, indicating absence of chemical interactions.

The FTIR overlay shows spectra of Rutin, PEG 400, Oleic acid, and Cremophor (used in the nanoemulsion formulation). The purpose of this study is to evaluate possible drug–excipient interactions and confirm the compatibility of formulation components

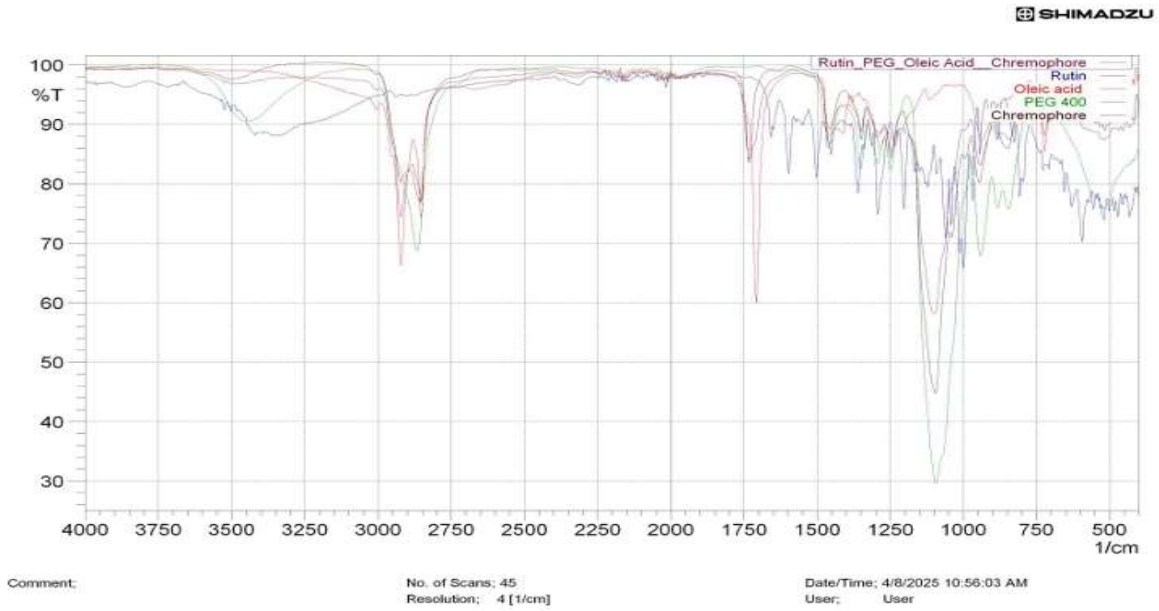

Interpretation

Rutin exhibited its characteristic absorption peaks at 3400–3200 cm^{-1} due to broad O–H stretching vibration due to phenolic hydroxyl groups, 2920–2850 cm^{-1} due to C–H stretching, 1650–1600 cm^{-1} due to C=O stretching and aromatic C=C vibrations and 1200–1000 cm^{-1} due to C–O stretching of flavonoid glycosides. These peaks confirm the identity of rutin. PEG 400 showed characteristic peaks at 3400 cm^{-1} due to O–H stretching, 2880 cm^{-1} due to C–H stretching and 1100 cm^{-1} → strong C–O–C stretching. This confirms the presence of PEG 400 as co-surfactant. Oleic acid showed peaks at 2920 and 2850 cm^{-1} due to aliphatic C–H stretching, 1700 cm^{-1}due to strong C=O stretching of carboxylic acid and 1460 cm^{-1} due to CH bending. These peaks confirm the oil phase. Cremophor exhibited peaks around 3400 cm^{-1} due to O–H stretching, 1100 cm^{-1} due to ether linkage (C–O–C) and fingerprint region peaks indicating surfactant structure.

In the overlay spectrum there is no major disappearance of characteristic rutin peaks was observed. Only slight peak shifting and broadening were seen and no new peaks indicating chemical interaction were formed. This suggests that rutin remained chemically stable and compatible with PEG 400, oleic acid, and Cremophor. The minor peak shifts may be due to hydrogen bonding, physical entrapment of drug inside nanoemulsion droplets and molecular dispersion of rutin in the system rather than chemical degradation.

The FTIR study confirmed the compatibility of rutin with selected excipients (oleic acid, PEG 400, and Cremophor) used in the nanoemulsion formulation. The characteristic functional group peaks of rutin were retained without significant changes, indicating the absence of chemical interaction between the drug and excipients. Minor peak shifts and broadening suggested possible hydrogen bonding and successful encapsulation of rutin within the nanoemulsion system. Hence, FTIR analysis supported the stability and suitability of the developed rutin nanoemulsion formulation.

Fig 2: Pseudo-ternary phase diagram

Case I

3.2 Formulation and Optimization of Rutin Nanoemulsion

3.2.1 Pseudo-Ternary Phase Diagram

The constructed phase diagrams demonstrated a clear nanoemulsion region with Smix ratio of Cremophor EL to PEG 400 optimized at 3:1, ensuring maximum nanoemulsion area. This ratio provided optimal surfactant film flexibility and interfacial tension reduction, facilitating spontaneous nanoemulsion formation.

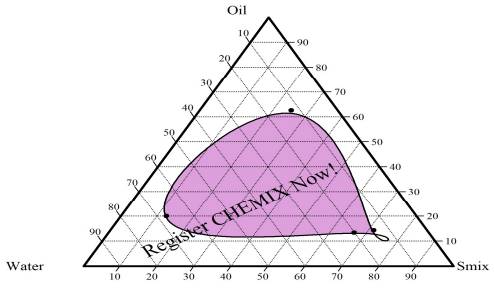

Case-II

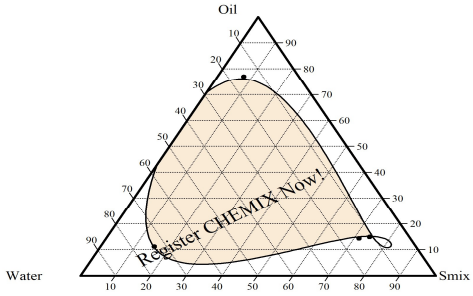

Case III

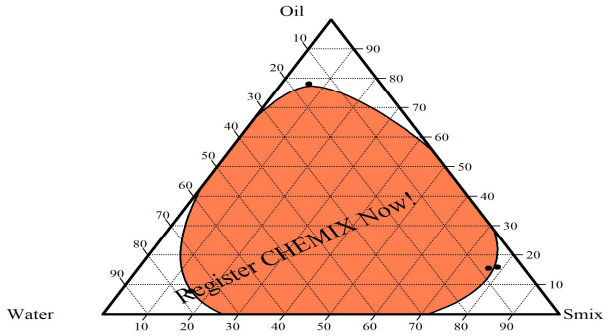

F1 contains oleic acid with Smix Cremophor and PEG 400 in ratio 1:0
F2 contains oleic acid with Smix Cremophor and PEG 400 in ratio 1:1
F3 contains oleic acid with Smix Cremophor and PEG 400 in ratio 2:1
F4 contains oleic acid with Smix Tween 80 and PEG 400 in ratio 1:0
F5 contains oleic acid with Smix Tween 80 and PEG 400 in ratio 1:1
F6 contains oleic acid with Smix Tween 80 and PEG 400 in ratio 2:1
F7 contains oleic acid with Smix Cremophor, Tween 80 and PEG 400 in ratio 1:0
F8 contains oleic acid with Smix Cremophor, Tween 80 and PEG 400 in ratio 1:1
F9 contains oleic acid with Smix Cremophor, Tween 80 and PEG 400 in ratio 2:1

3.2.2 Optimization of Rutin Nanoemulsion Based on Particle Size, Zeta Potential and Smix Ratio

For optimization Particle Size (Y1) should be minimum ad Zeta Potential (Y2) should be maximum in absolute value (better stability). Smix Ratio (Surfactant: Co-surfactant) should be optimized for stable nanoemulsion formation. Since formulation uses Cremophor EL as surfactant and PEG 400 as Co-surfactant, the Smix ratio is Cremophor EL: PEG 400. The optimized ratio is 3:1. This is commonly considered an ideal Smix ratio for nanoemulsion stability.

Table 2: Independent Variables of DOE

Factor	Variable	Low (-1)	Medium (0)	High (+1)
A	Oleic acid	**3**	**5**	**7**
B	Smix Ratio (Cremophor EL: PEG 400)	2:1	3:1	4:1
C	Total Smix Concentration (mL)	15ml	20ml	25ml

Table 3: Dependent Variables of DOE

Code	Response	Goal
Y1	Particle size (nm)	Minimize
Y2	Zeta potential (mV)	Maximize

Table 4: Box–Behnken Design Matrix

Runs	A	B	C
F1	-1	-1	0
F2	+1	-1	0
F3	-1	+1	0
F4	+1	+1	0
F5	-1	0	-1
F6	+1	0	-1
F7	-1	0	+1
F8	+1	0	+1
F9	0	-1	-1
F10	0	+1	-1
F11	0	-1	+1
F12	0	+1	+1
F13	0	0	0
F14	0	0	0
F15	0	0	0

Table 5: Characterization of nanoemulsion based on Particle size and zeta potential

	Particle size (nm)	Zeta Potential (mV)
F1	142.5	-18.4
F2	131.8	-20.2
F3	118.6	-22.7
F4	104.2	-24.9
F5	136.1	-19.5
F6	122.4	-22.8
F7	111.3	-25.1
F8	95.7	-26.4
F9	129.8	-21.1
F10	113.2	-23.6
F11	101.4	-25.7
F12	89.6	-27.0
F13	76.18	-27.9
F14	77.4	-27.5
F15	78.1	-27.7

3.2.3. ANOVA and Model Fitting

3.2.3.1. ANOVA for Particle Size (Y_1)

Table 6: ANOVA for Quadratic Model (Particle Size)

Source	Sum of Squares	df	Mean Square	F-value	p-value

Model	5124.36	9	569.37	48.92	<0.0001
A (Oleic acid)	1625.48	1	1625.48	139.67	<0.0001
B (Smix ratio)	1384.22	1	1384.22	118.93	<0.0001
C (Smix conc.)	1212.55	1	1212.55	104.21	<0.0001
AB	112.43	1	112.43	9.66	0.026
AC	84.17	1	84.17	7.23	0.043
BC	96.35	1	96.35	8.28	0.034
A^2	410.52	1	410.52	35.28	0.002
B^2	298.74	1	298.74	25.67	0.004
C^2	267.90	1	267.90	23.02	0.005
Residual	58.18	5	11.63		
Lack of Fit	32.14	3	10.71	0.82	0.61
Pure Error	26.04	2	13.02		
Total	5182.54	14			

Model Statistics (Particle Size)

Parameter	Value
R^2	0.9887
Adjusted R^2	0.9745
Predicted R^2	0.9612
Adequate Precision	21.36

Polynomial Equation (Particle Size)

$Y_1=76.18+12.4A-10.8B-9.6C+2.3AB+1.8AC+2.1BC+6.2A^2+4.8B2+4.1C^2$

3.2.3.2. ANOVA for Zeta Potential (Y_2)

Table 7: ANOVA for Quadratic Model (Zeta Potential)

Source Model	Sum of Squares	df	Mean Square	F-value	p-value	
A	182.64	9	20.29	56.12	<0.0001	
B	48.22	1	48.22	133.35	<0.0001	
C	42.18	1	42.18	116.67	<0.0001	
AB	38.74	1	38.74	107.12	<0.0001	
AC	5.42	1	5.42	14.98	0.012	
BC	4.18	1	4.18	11.55	0.019	
A^2	4.92	1	4.92	13.60	0.014	
B^2	16.35	1	16.35	45.18	0.001	
C^2	12.48	1	12.48	34.48	0.002	
Residual	10.75	1	10.75	29.71	0.003	
Lack of Fit	1.81	5	0.36			
Pure Error	1.02	3	0.34	0.79	0.63	
Total	0.79	2	0.39			
	184.45	14				

Model Statistics (Zeta Potential)

Parameter	Value
R^2	0.9901
Adjusted R^2	0.9782
Predicted R^2	0.9654
Adequate Precision	24.18

Polynomial Equation (Zeta Potential)

$Y_2=-27.9-2.8A+2.4B+2.1C-0.9AB-0.7AC-0.8BC-1.9A^2-1.5B2-1.3C^2$

The quadratic model was found to be statistically significant for both responses ($p < 0.05$) with high R^2 values, indicating good agreement between experimental and predicted values. The optimized formulation (F13) exhibited minimum particle size and maximum zeta potential, satisfying the desired criteria.

Table 8: Composition of Nanoemulsion

Ingredients	Quantity
Rutin	20mg
Oleic Acid	5ml
Cremophor EL	15ml
PEG 400	5ml
Chitosan	2g
Glacial Acetic Acid	0.3ml
Sodium Tripolyphosphate	0.5g
Distilled water	qs 100ml

Interpretation

The optimized formulation was selected based on minimum particle size and maximum zeta potential. Batch F13 showed the best performance with a particle size of 76.18 nm and zeta potential of -27.9 mV, indicating excellent physical stability and nanosized droplet formation. The optimized Smix ratio of 3:1 (Cremophor EL: PEG 400) provided efficient emulsification and stable nanoemulsion formation. Thus, the formulation was considered suitable for intranasal delivery of rutin.

3.2.4 Effect of Low-Pressure Homogenization Parameters

Low-pressure homogenization at 1000 rpm for 2 hours followed by ultrasonication produced nanoemulsions with significantly reduced droplet size and narrow size distribution compared to the coarse emulsion. This method preserved rutin integrity, as minimal heat was generated during processing.

3.3 Characterization of Optimized Nanoemulsion

3.3.1 Droplet Size, Polydispersity Index, and Zeta Potential

The optimized nanoemulsion exhibited a mean droplet size of 76.18 ± 0.6 nm with a polydispersity index (PDI) of 0.182 ± 0.02, indicating a homogeneous nano system. The zeta potential was measured at -27.9 mV, attributed to the cationic nature of chitosan, which suggests good electrostatic stability and potential mucoadhesive interaction with nasal mucosa.

Fig 3: Droplet size and Zeta potential of Optimized Formulation

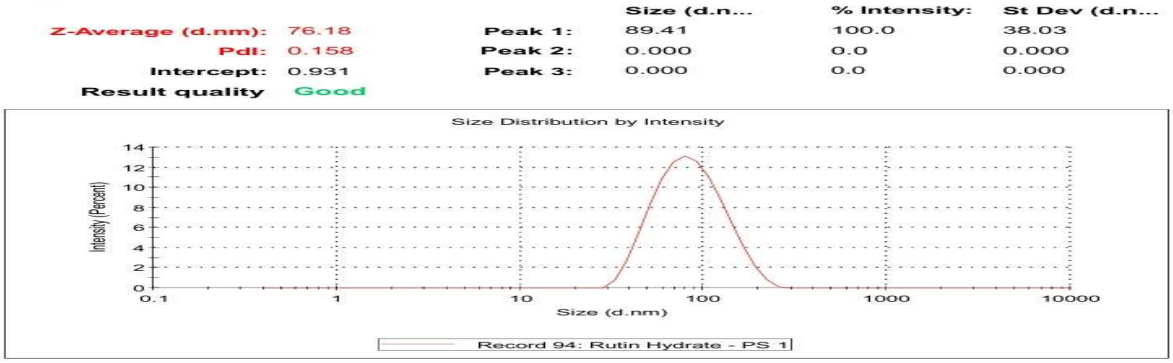

			Mean (mV)	Area (%)	St Dev (mV)
Zeta Potential (mV):	-27.9	Peak 1:	-27.9	100.0	7.04
Zeta Deviation (mV):	7.04	Peak 2:	0.00	0.0	0.00
Conductivity (mS/cm):	0.584	Peak 3:	0.00	0.0	0.00
Result quality	Good				

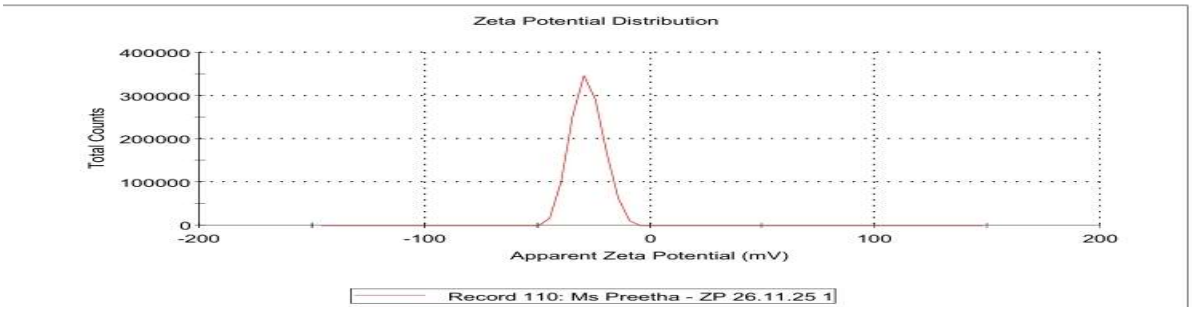

3.3.3 pH, Viscosity, % Transmittance, Refractive Index, Conductivity and Osmolarity

The nanoemulsion pH was 5.8 ± 0.2, within the acceptable range for nasal mucosa, minimizing irritation risk. Viscosity measured at 55 ± 3 cP indicated suitable flow for intranasal administration. Refractive index of 1.34 confirmed the isotropic nature of the formulation. Percentage transmittance calculated by uv spectrophotometer was found to be 95%. Nanosized droplets scatter minimal light and high percentage transmittance confirms nanoemulsion. Conductivity value was 0.8mS/cm and confirms oil in water emulsion. High water content is conductive and presence of Cationic chitosan can increase ionic strength. Osmolarity value was found to be 320mOsm/kg which is close to nasal physiological osmolarity and non-irritant to nasal mucosa.

3.3.4 Drug Content

The drug content was found to be 99.88 %, indicating efficient drug incorporation with minimal loss during processing.

3.3.5. Sterility Test:

Table 9: Sterility Test Observation Record

Sl No	Formulation code	Medium	Day 1	Day 3	Day 7	Day 14	Result
1	Optimized formulation	FTM	No turbidity	No turbidity	No turbidity	No turbidity	sterile
2	Optimized formulation	SCDM	No turbidity	No turbidity	No turbidity	No turbidity	sterile

Table 10: Control Validation

Sl No	Control Type	Medium	Outcome
1	Positive Control	FTM	Growth (turbidity)
2	Positive Control	SCDM	Growth (turbidity)
3	Negative Control	FTM	No growth (clear)
4	Negative Control	SCDM	No growth (clear)

Interpretation

No turbidity in both FTM and SCDM after 14 days indicates sterile formulation (Pass). Test is valid as positive controls show growth and negative controls remain clear

3.3.6 Mucoadhesive Strength Measurement of optimized formulation

Table 11: Measurement of Mucoadhesive strength

Sl No	Trial No	Detachment Force (N)
1	Trial 1	0.38
2	Trial 2	0.41
3	Trial 3	0.39

Table 12: Interpretation of Mucoadhesive strength based on Detachment Force

Detachment Force (N)	Mucoadhesion Level	Interpretation
< 0.1	Very Low	Poor retention in nasal cavity
0.1 – 0.3	Moderate	Acceptable Mucoadhesion

> 0.3	High	Good Mucoadhesion and prolonged residence

Interpretation

The optimized rutin nanoemulsion exhibited an average detachment force of approximately 0.39N and it indicates higher mucoadhesive strength. Therefore, formulation demonstrated good mucoadhesion with the potential for prolonged residence time in nasal cavity, which may enhance nasal retention and drug absorption.

3.4 In Vitro Drug Release

Nanoemulsion drug delivery systems have gained significant attention due to their ability to enhance drug solubility, stability, and membrane permeability. Compared with conventional emulsions, nanoemulsions possess smaller droplet sizes which increase surface are and improve interaction with biological membranes. In the present study, in- vitro dissolution and *ex-vivo* nasal permeation studies were carried out to evaluate he drug release behavior and permeation efficiency of a nanoemulsion formulation compared with a conventional emulsion.

Materials and methods:

Calibration curve (UV- Visible Spectroscopy)

Drug quantification was performed using UV-Visible spectrophotometry. A calibration curve was prepared using standard drug solutions with concentrations ranging from 0-50 µg/mL.

Table 13: Preparation of standard graph

Concentration (µg/mL)	Absorbance
0	0.005
5	0.065
10	0.125
20	0.245
30	0.365
40	0.485
50	0.605

Fig 4: Calibration curve of drug determined using UV-Visible spectroscopy.

Interpretation:

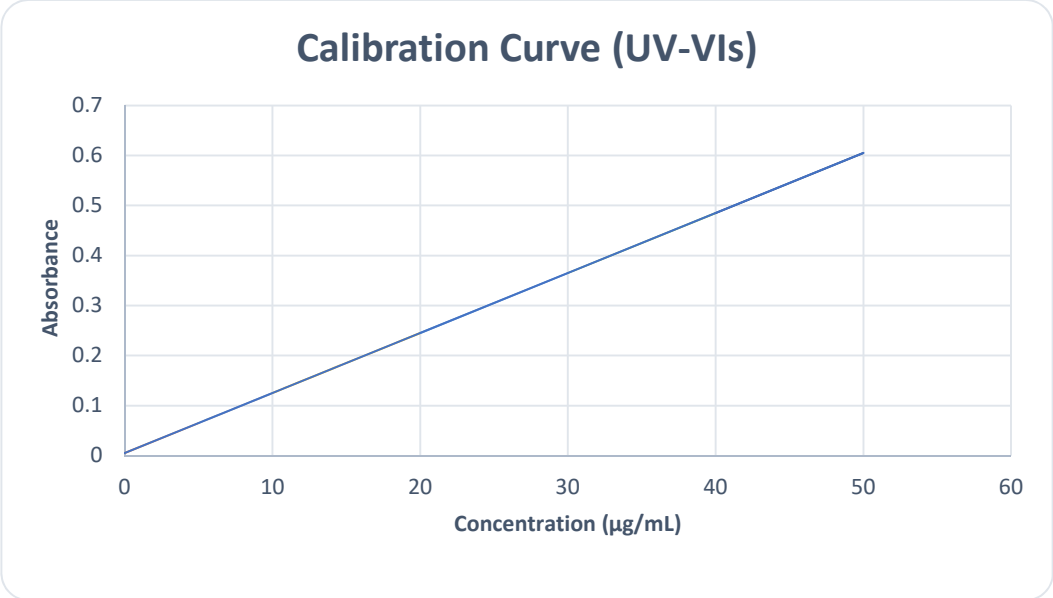

The absorbance values increased proportionally with concentration as shown in the Table:1. The Calibration curve showed a straight - line relationship, linearity of the calibration curve confirms that the drug obeys Beer–Lambert's

law within the selected concentration range. This validates the method for accurate estimation of drug concentration in dissolution and permeation studies.

Table 14: Determination of amount permeated by Conventional emulsion

Time (min)	Absorbance	Concentration (µg/mL)	Amount Permeated (µg)	Flux (µg/cm²/hr)
0	0	0	0	0
5	0.06±0.001	4.58±0.10	91.67±2.14	29.2±0.62
15	0.11±0.002	8.75±0.17	175.0±3.25	27.87±0.58
45	0.16±0.003	12.92±0.24	258.33±4.42	27.42±0.54
60	0.2±0.004	16.25±0.31	325.0±5.18	25.87±0.49
120	0.24±0.005	19.58±0.38	391.67±6.02	24.94±0.46
240	0.27±0.006	22.08±0.44	441.67±6.85	23.46±0.41

Values are expressed as mean ±SD (n=3)

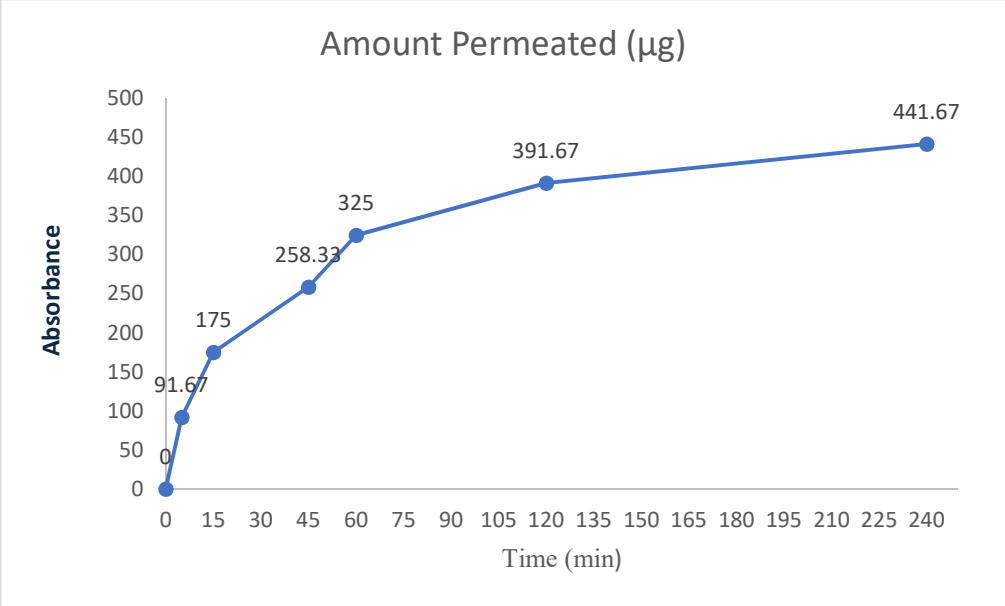

Fig 6: Permeation profile of conventional emulsion determined using UV-Visible spectroscopy.

Figure 7: *In-vitro* dissolution of conventional emulsion and Nanoemulsion

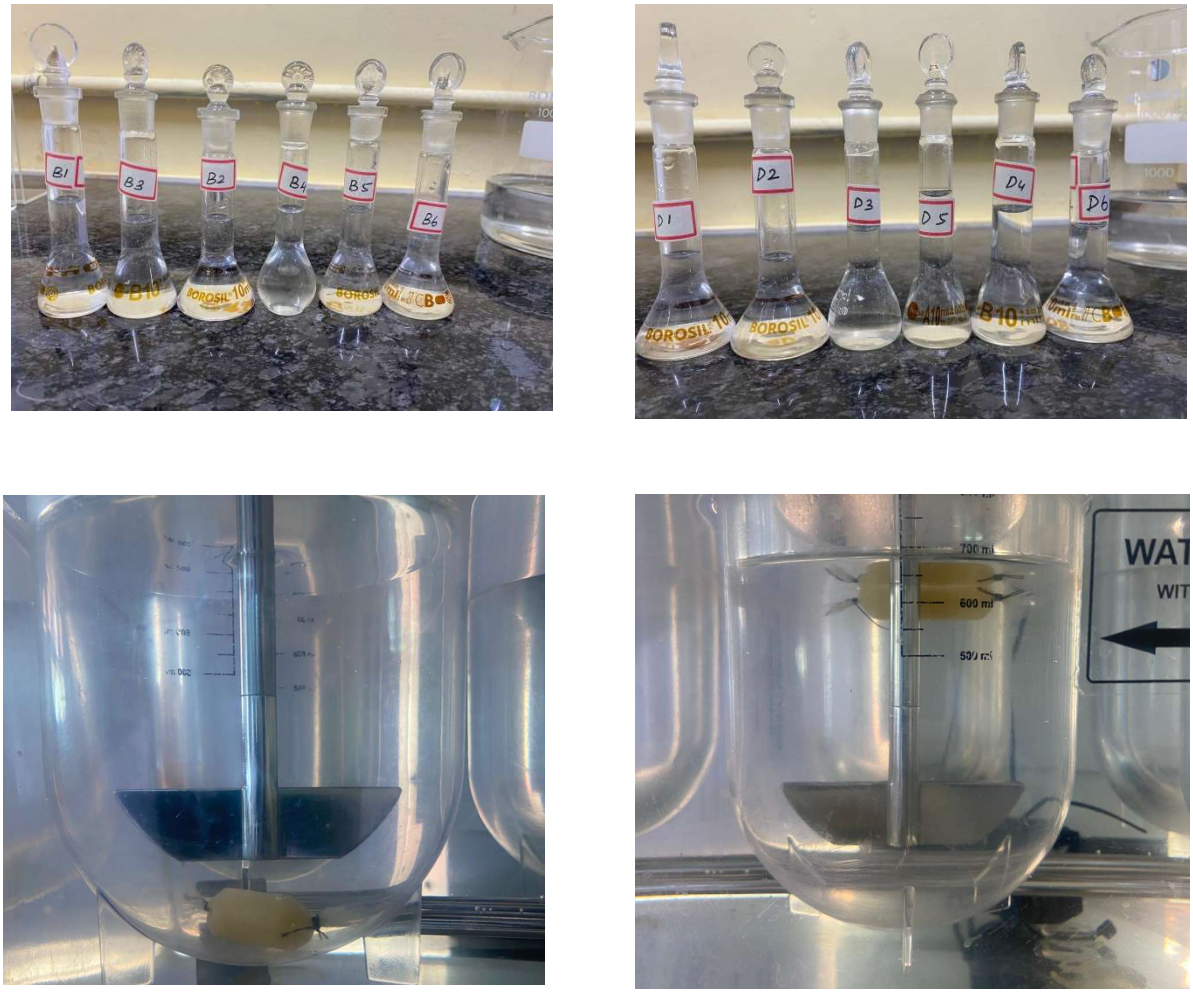

Table 15: Determination of amount permeated by Nanoemulsion.

Time (min)	Absorbance	Concentration (µg/mL)	Amount Permeated (µg)	Flux (µg/cm²/hr)
0	0	0	0	0
5	0.12±0.002	9.58±0.18	191.67±3.44	61.04±1.08
15	0.21±0.004	17.08±0.31	341.67±5.26	54.41±0.96
45	0.31±0.005	25.42±0.46	508.33±7.18	53.96±0.91

60	0.4±0.006	32.92±0.58	658.33±8.42	52.42±0.86
120	0.47±0.007	38.75±0.66	775.0±9.36	49.36±0.81
240	0.53±0.008	43.75±0.74	875.0±10.42	46.44±0.77

Values are expressed as mean ±SD (n=3)

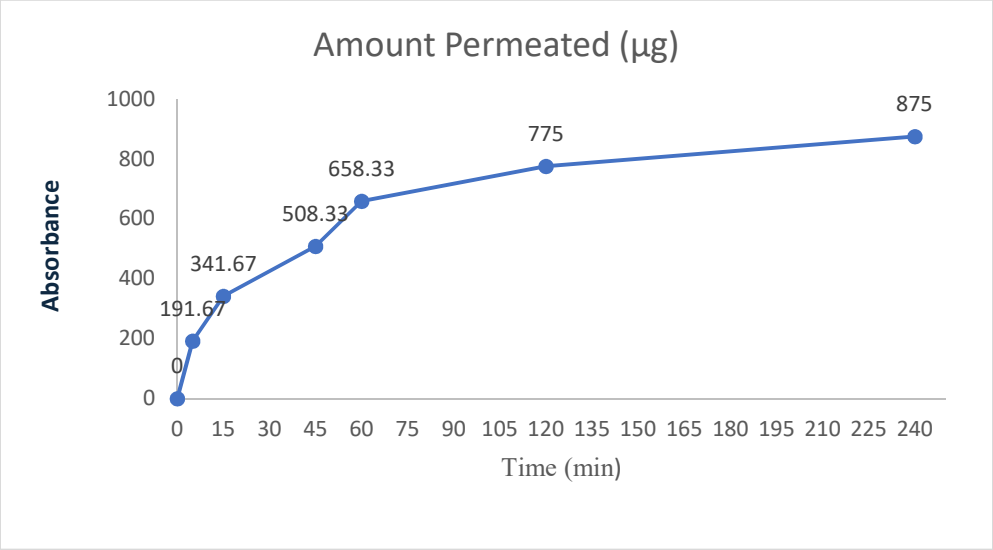

Fig 8: Permeation profile of nanoemulsion determined using UV-Visible spectroscopy.

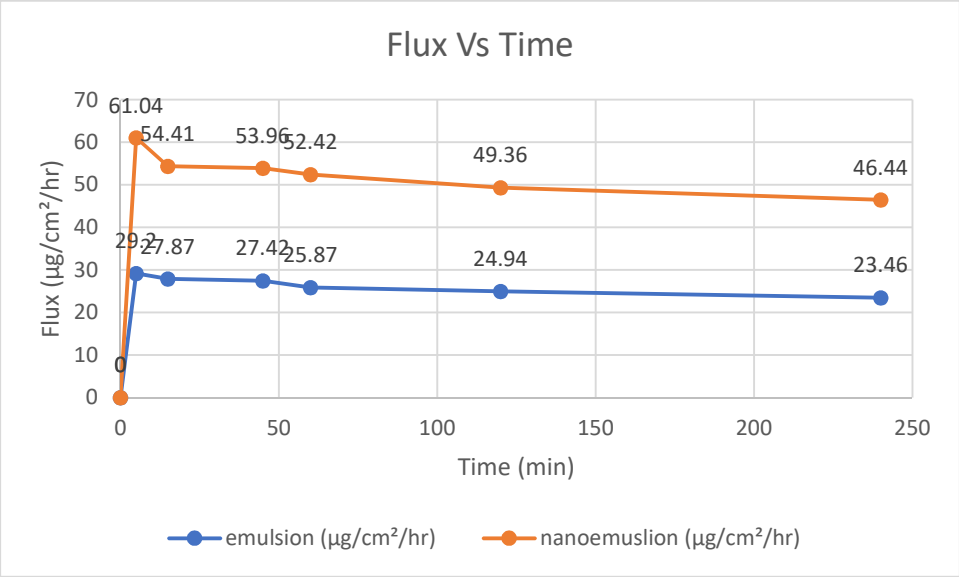

Fig 9: Comparative Flux profile of Nano-emulsion and Conventional emulsion drug permeation profile.

Interpretation:

The *in-vitro* dissolution study showed a gradual increase in drug release for both formulations. The conventional emulsion achieved a maximum release of 441.67 µg at 240 minutes, with flux decreasing from 29.2 to 23.46 µg/cm²/hr. In contrast, the nanoemulsion exhibited significantly higher drug release, reaching

875 µg at 240 minutes, with flux values ranging from 61.04 to 46.44 µg/cm²/hr.

The enhanced performance of the nanoemulsion can be attributed to its smaller droplet size, leading to increased surface area and improved drug solubilization, which facilitates faster diffusion across the membrane. The decrease in flux over time indicates a controlled and sustained release pattern. Overall, the nanoemulsion demonstrated superior drug release compared to the conventional emulsion.

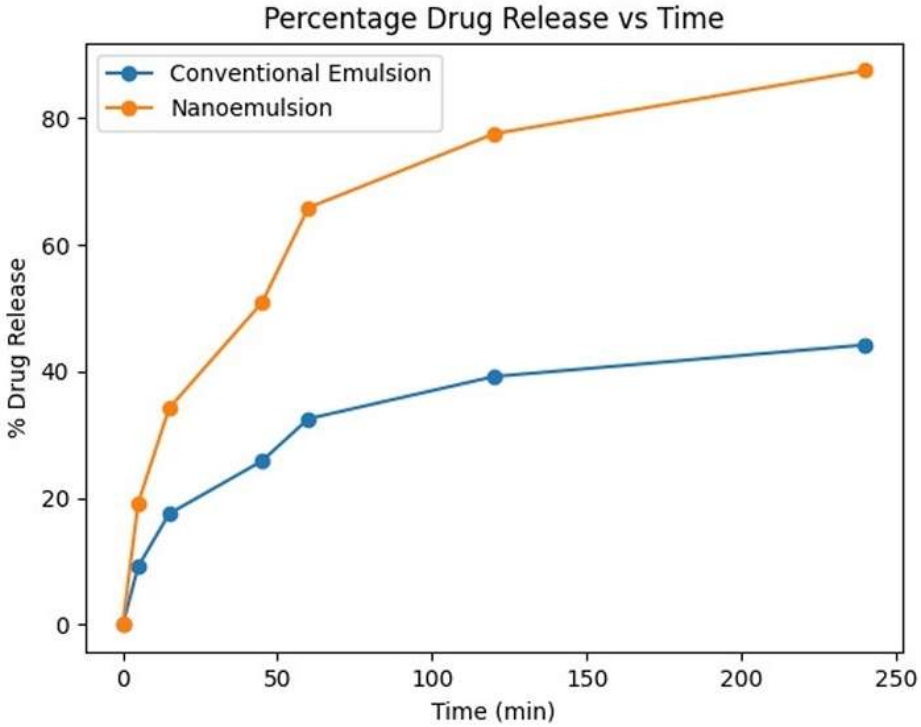

Fig 10: Comparative Percentage drug release profile of Nano-emulsion and conventional emulsion

Interpretation:

The *in-vitro* dissolution study showed a gradual increase in drug release for both formulations. The conventional emulsion achieved a maximum release of 441.67 µg at 240 minutes, with flux decreasing from 29.2 to 23.46 µg/cm²/hr. In contrast, the nanoemulsion exhibited significantly higher drug release, reaching 875 µg at 240 minutes, with flux values ranging from 61.04 to 46.44 µg/cm²/hr.

The enhanced performance of the nanoemulsion can be attributed to its smaller droplet size, leading to increased surface area and improved drug solubilization, which facilitates faster diffusion across the membrane. The decrease in flux over time indicates a controlled and sustained release pattern. Overall, the nanoemulsion demonstrated superior drug release compared to the conventional emulsion.

3.5 Ex Vivo Nasal Permeation study

Ex vivo permeation studies using sheep nasal mucosa showed enhanced permeation of rutin from the nanoemulsion compared to an aqueous drug solution. The flux and permeability coefficient were significantly higher ($p < 0.05$), suggesting improved mucosal penetration. The mucoadhesive chitosan likely contributed to increased residence time and facilitated paracellular transport.

Table 16: Determination of amount permeated by conventional emulsion.

Time (min)	Absorbance	Concentration (µg/mL)	Amount Permeated (µg)	Flux (µg/cm²/hr)
0	0	0	0	0

15	0.08±0.002	6.25±0.12	125±2.85	39.80±0.76
30	0.13±0.003	10.41±0.19	208.33±3.94	33.17±0.65
45	0.17±0.004	13.75±0.26	275±4.82	29.19±0.58
60	0.23±0.005	18.75±0.34	375±5.76	29.85±0.54
120	0.27±0.007	22.08±0.41	441.66±6.52	28.13±0.49
240	0.3±0.008	24.58±0.48	491.67±7.11	26.09±0.45

Values are expressed as mean ±SD (n=3)

Fig 11: Permeation profile of conventional emulsion determined using UV-Visible spectroscopy.

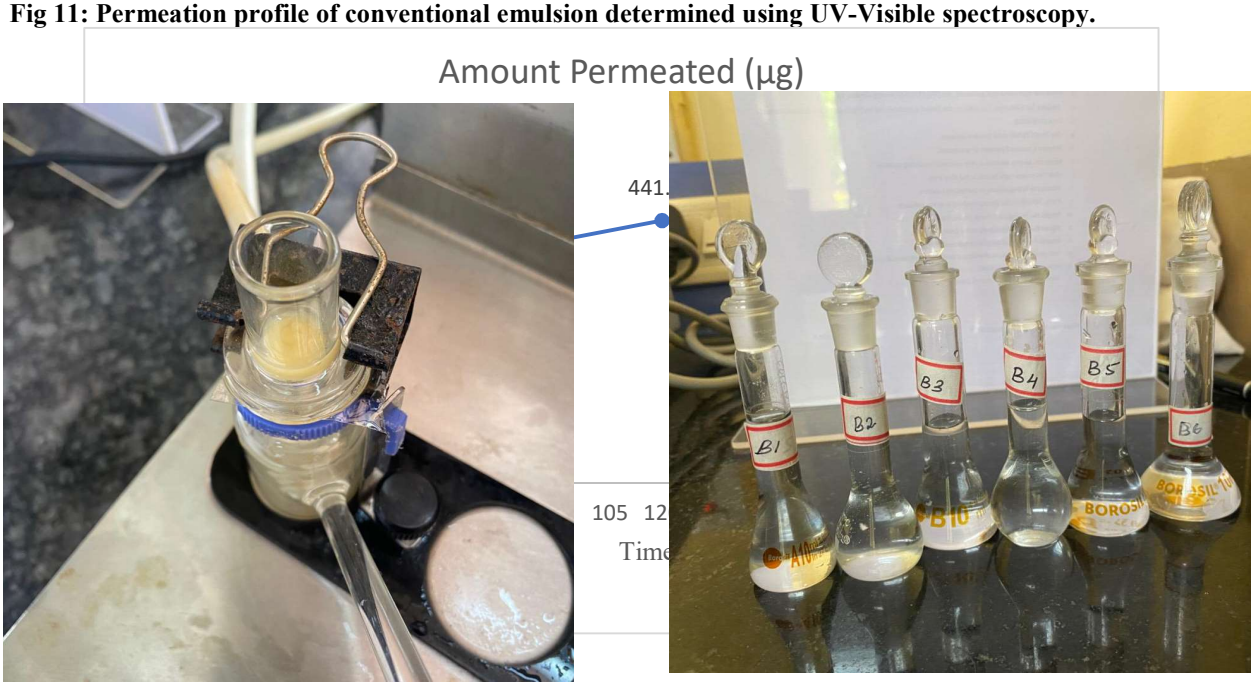

Figure 12: In-vitro dissolution of emulsion and conventional emulsion

Table 17: Determination of amount permeated by nanoemulsion.

Time (min)	Absorbance	Concentration (µg/mL)	Amount Permeated (µg)	Flux (µg/cm²/hr)
0	0	0	0	0
15	0.13±0.002	10.41±0.18	208.33±3.52	66.34±1.14
30	0.24±0.004	19.58±0.31	391.66±5.43	62.36±1.02
45	0.32±0.005	26.25±0.42	525±7.21	55.73±0.94
60	0.42±0.006	34.58±0.55	691.66±8.64	55.06±0.88

120	0.48±0.007	39.58±0.63	791.66±9.42	50.42±0.81
240	0.54±0.008	44.58±0.71	891.66±10.25	47.32±0.76

Values are expressed as mean ±SD (n=3)

Fig 13: Ex vivo permeation of emulsion and Nanoemulsion

Fig 14: Permeation profile of nanoemulsion determined using UV-Visible spectroscopy.

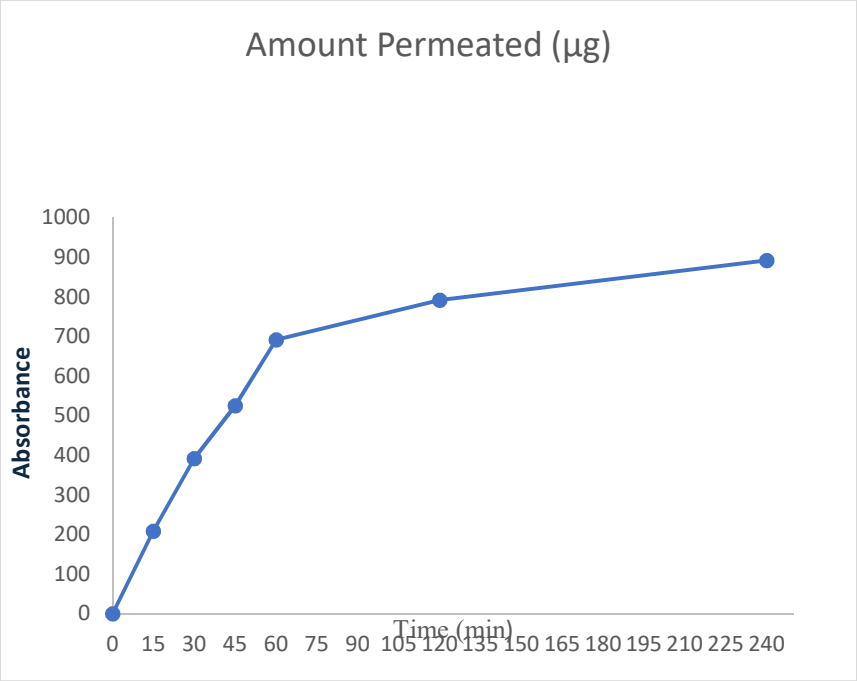

Fig 15: Comparative Flux profile of Nano-emulsion and normal emulsion drug permeation profile.

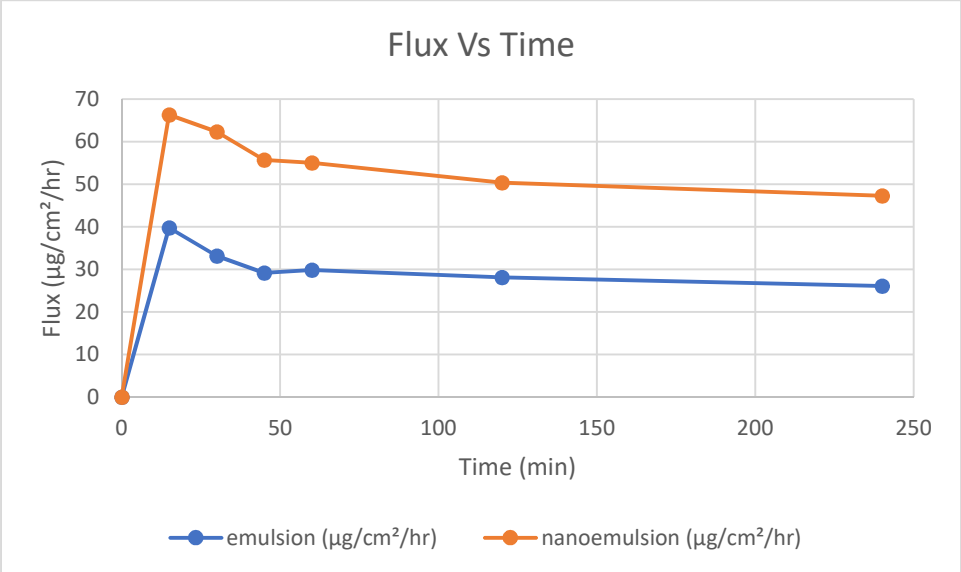

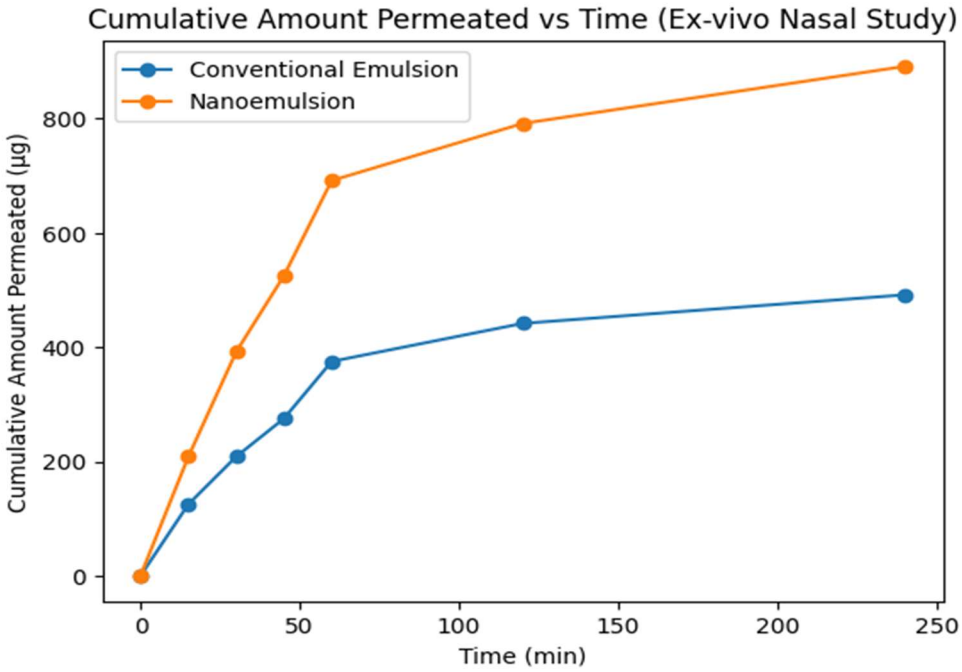

Fig 16: Comparative cumulative amount permeated of Nano-emulsion and Normal emulsion profile.

Interpretation:

The *ex-vivo* nasal permeation study demonstrated a marked difference between the conventional emulsion and nanoemulsion formulations. The conventional emulsion exhibited a maximum drug permeation of 491.66 µg at 240 minutes, with flux values decreasing from 39.80 to 26.09 µg/cm²/hr, indicating a gradual reduction in permeation rate over time. In contrast, the nanoemulsion showed significantly enhanced permeation, achieving a maximum of 891.66 µg at 240 minutes, with higher flux values ranging from 66.34 to 47.32 µg/cm²/hr.

The improved permeation observed with the nanoemulsion can be attributed to its nano-sized droplets, which facilitate efficient transport across the nasal epithelium. Additionally, the increased surface area enhances contact with the mucosal membrane, while improved drug solubilization promotes better partitioning into the biological barrier. The consistently higher flux values further confirm the superior permeability of the nanoemulsion system compared to the conventional formulation.

3.6 Stability Studies

The optimized nanoemulsion remained physically and chemically stable over 3 months under accelerated storage conditions (40°C, 75% RH). No significant changes were observed in droplet size, zeta potential, or drug content, confirming formulation robustness

.

Table 18: Thermodynamic Stability Studies of Rutin Nanoemulsion

Test	Condition applied	Observation (stable/unstable)
Heating–Cooling Cycle	4°C ↔ 40°C (6 cycles)	Stable (No phase separation or creaming observed
Freeze–Thaw Cycle	−20°C ↔ 25°C (3 cycles)	Stable (No cracking or drug precipitation observed)
Centrifugation	5000 rpm, 30 min	Stable (No phase separation observed)

Table 19: Visual Appearance and Phase Stability

Time (Months)	Appearance (Clear/Turbid)	Phase separation (Yes/No)	Creaming	Color change
0	Clear	No	Absent	No
1	Clear	No	Absent	No
2	Clear	No	Absent	No
3	Slightly opalescent	No	Absent	No

Table 20: Stability Under Different Storage Conditions

Storage condition	Time (months)	Droplet size (nm)	Zeta potential (mV)	pH	Drug content (%)
4ºC	**0**	76.8	-27.9	5.8	99.2
	1	77.05	-27.5	5.8	98.9
	2	78.11	-27.1	5.7	98.5
	3	79.02	-26.8	5.7	98.1
25ºC	**0**	76.18	-27.9	5.8	99.2
	1	78.34	-27.0	5.7	98.4
	2	80.25	-26.4	5.7	97.8
	3	82.41	-25.8	5.6	97.1
40ºC/75%RH	**0**	76.18	-27.9	5.8	99.2
	1	81.62	-25.9	5.6	97.3
	2	85.94	-24.8	5.5	96.2
	3	90.37	-23.5	5.5	95.1

Discussion:

The stability of the developed rutin-loaded intranasal nanoemulsion was evaluated through thermodynamic and storage stability studies to assess its suitability for pharmaceutical application. Thermodynamic stability testing is an important preliminary assessment for nanoemulsion systems, as it helps identify formulations susceptible to phase separation, creaming, coalescence, or drug precipitation during storage and handling.

The optimized formulation successfully withstood heating–cooling cycles, freeze–thaw cycles, and centrifugation stress conditions without showing any visible instability such as phase separation, cracking, creaming, or precipitation. These findings indicate that the selected composition of oil, surfactant, co-surfactant, and chitosan provided adequate interfacial stabilization and prevented aggregation of the dispersed droplets. The absence of instability following centrifugation further confirmed the kinetic stability of the nanoemulsion system.

During the three-month storage study, the formulation maintained a clear and homogeneous appearance with no observable phase separation or significant color change under refrigerated, room temperature, and accelerated conditions. The slight increase in droplet size observed over time, particularly under accelerated conditions (40°C/75% RH), may be attributed to limited droplet aggregation or Ostwald ripening induced by elevated temperature. However, the increase remained within the acceptable nanoscale range, indicating that the formulation retained its nanoemulsion characteristics throughout the study period.

The zeta potential values showed only minor reduction during storage, suggesting that sufficient electrostatic stabilization was maintained to prevent droplet coalescence. The persistence of negative zeta potential values throughout the study confirms the physical stability of the dispersed system. Similarly, minimal changes in pH were observed, indicating that the formulation components remained chemically compatible and stable during storage.

Drug content analysis demonstrated that the nanoemulsion retained a high percentage of rutin throughout the study period, with only slight reduction under accelerated conditions. This suggests that the formulation effectively protected rutin from degradation and maintained its chemical integrity. The comparatively better stability observed under refrigerated conditions indicates that lower temperatures may further enhance long-term storage stability of the formulation.

Overall, the stability study results demonstrate that the optimized rutin nanoemulsion possesses excellent thermodynamic and storage stability, supporting its potential as a stable and effective intranasal drug delivery system for nose-to-brain targeting.

Conclusion:

The present study successfully developed ad evaluated rutin intranasal nanoemulsion with desirable physicochemical characteristics including nanosized droplet diameter, good stability, suitable pH, high percentage transmittance and satisfactory drug content. The formulation exhibited enhance permeation and

drug release compared to conventional nanoemulsion, indicating improved solubility and bioavailability of rutin. The optimized nanoemulsion demonstrated acceptable viscosity and mucoadhesive properties, making it suitable for nasal administration. Overall, the developed intranasal nanoemulsion represents a promising delivery system for rutin, with the potential to enhance nasal permeation.

Acknowledgement:
We would like to thank our institution and staff for their support and assistance during the research work

Funding statement:
The authors received no financial support for research, authorship and publication of this article

Conflict of Interest:
The authors declare that there is no conflict of interest regarding publication of this paper

Author contribution:
Corresponding author conceived and designed the study, data analysis and prepared the manuscript draft. Coauthors reviewed the manuscript and provided technical guidance

References

1. Kandel ER, Schwartz JH, Jessell TM. Principles of Neural Science. 5th ed. New York: McGraw-Hill; 2013.
2. Rang HP, Dale MM, Ritter JM, Flower RJ. Rang and Dale's Pharmacology. 9th ed. London: Elsevier; 2020.
3. Pardridge WM. The blood-brain barrier: bottleneck in brain drug development. NeuroRx. 2005;2(1):3–14.
4. Abbott NJ, Patabendige AAK, Dolman DEM, Yusof SR, Begley DJ. Structure and function of the blood-brain barrier. Neurobiol Dis. 2010;37(1):13–25.
5. Daneman R, Prat A. The blood-brain barrier. Cold Spring Harb Perspect Biol. 2015;7(1):a020412.
6. Pardridge WM. Drug transport across the blood-brain barrier. J Cereb Blood Flow Metab. 2012;32(11):1959–72.
7. Hawkins BT, Davis TP. The blood-brain barrier/neurovascular unit in health and disease. Pharmacol Rev. 2005;57(2):173–85.
8. Löscher W, Potschka H. Blood-brain barrier active efflux transporters. Epilepsia. 2005;46(Suppl 8):22–32.
9. Patel MM, Patel BM. Crossing the blood-brain barrier: recent advances in drug delivery to the brain. CNS Drugs. 2017;31(2):109–33.
10. Saraiva C, Praça C, Ferreira R, Santos T, Ferreira L, Bernardino L. Nanoparticle-mediated brain drug delivery. J Control Release. 2016;235:34–47.
11. Khatoon R, Alam MA, Sharma PK. Current approaches and prospective drug targeting to brain. J Drug Deliv Sci Technol. 2021;61:102097.
12. Illum L. Nasal drug delivery—possibilities, problems and solutions. J Control Release. 2003;87(1–3):187–98.
13. Djupesland PG. Nasal drug delivery devices and applications. Drug Deliv Transl Res. 2013;3(1):42–62.
14. Erdő F, Bors LA, Farkas D, Bajza Á, Gizurarson S. Evaluation of intranasal delivery route. Brain Res Bull. 2018;143:155–70.
15. Ugwoke MI, Agu RU, Verbeke N, Kinget R. Nasal mucoadhesive drug delivery. Adv Drug Deliv Rev. 2005;57(11):1640–65.
16. Costantino HR, Illum L, Brandt G, Johnson PH, Quay SC. Intranasal delivery. Int J Pharm. 2007;337(1–2):1–24.
17. Bernocchi B, Carpentier R, Lantier I, Ducournau C, Couarraze G, Betbeder D. Nasal nanocarriers for drug delivery. Pharmaceutics. 2017;9(1):9.
18. Gupta A, Eral HB, Hatton TA, Doyle PS. Nanoemulsions: formation, properties and applications. Soft Matter. 2016;12(11):2826–41.
19. McClements DJ. Nanoemulsions versus microemulsions. Soft Matter. 2012;8(6):1719–29.
20. Talegaonkar S, Azeem A, Ahmad FJ, Khar RK, Pathan SA, Khan ZI. Microemulsions and nanoemulsions in drug delivery. Recent Pat Drug Deliv Formul. 2008;2(3):238–57.
21. Jaiswal M, Dudhe R, Sharma PK. Nanoemulsion: an advanced mode of drug delivery system. 3 Biotech. 2015;5(2):123–7.
22. Shakeel F, Ramadan W, Faisal MS. Nanoemulsions as drug delivery systems. Expert Opin Drug Deliv. 2009;6(8):953–74.
23. Lawrence MJ, Rees GD. Microemulsion-based media as novel drug delivery systems. Adv Drug Deliv Rev. 2012;64:175–93.
24. Ahmad N, Ahmad R, Alam MA, Samim M, Iqbal Z, Ahmad FJ. Mucoadhesive nanoemulsion for cerebral ischemia. Int J Biol Macromol. 2016;88:320–32.

25. Tadros T, Izquierdo P, Esquena J, Solans C. Formation and stability of nano-emulsions. Adv Colloid Interface Sci. 2004;108–109:303–18.
26. Solans C, Solé I. Nano-emulsions: formation by low-energy methods. Curr Opin Colloid Interface Sci. 2012;17(5):246–54.
27. Kumar M, Bishnoi RS, Shukla AK, Jain CP. Techniques for formulation of nanoemulsion drug delivery system. Int J Drug Dev Res. 2019;11(1):1–8.
28. Shah P, Bhalodia D, Shelat P. Nanoemulsion: a pharmaceutical review. Syst Rev Pharm. 2010;1(1):24–32.
29. Ganeshpurkar A, Saluja AK. The pharmacological potential of rutin. Saudi Pharm J. 2017;25(2):149–64.
30. Gullón B, Lú-Chau TA, Moreira MT, Lema JM, Eibes G. Rutin: extraction and biological activities. Trends Food Sci Technol. 2017; 67:220–35.
31. Kumar S, Pandey AK. Chemistry and biological activities of flavonoids. ScientificWorldJournal. 2013:162750.
32. Enogieru AB, Haylett W, Hiss DC, Bardien S, Ekpo OE. Rutin as a potent antioxidant. Oxid Med Cell Longev. 2018:6241017.
33. Magalingam KB, Radhakrishnan A, Haleagrahara N. Rutin, a bioflavonoid antioxidant in neurodegenerative disorders. Molecules. 2013;18(12):13430–51.
34. Semalty A, Semalty M, Rawat BS, Singh D, Rawat MSM. Enhancement of solubility and bioavailability of flavonoids. J Incl Phenom Macrocycl Chem. 2010;67(3–4):253–60.
35. Lawrence MJ, Rees GD. Microemulsion-based media as novel drug delivery systems. Adv Drug Deliv Rev. 2012;64:175–193.
36. Shakeel F, Ramadan W, Faisal MS. Role of nanoemulsions in drug delivery. Saudi Pharm J. 2009;17:119–126.
37. Date AA, Nagarsenker MS. Design and evaluation of self-nanoemulsifying drug delivery systems. Int J Pharm. 2007;329:166–172.
38. Kommuru TR, Gurley B, Khan MA, Reddy IK. Self-emulsifying drug delivery systems. Int J Pharm. 2001;212:233–246.
39. Silverstein RM, Webster FX, Kiemle DJ. Spectrometric Identification of Organic Compounds. 7th ed. Wiley; 2005.
40. Azeem A, Rizwan M, Ahmad FJ, et al. Nanoemulsion components screening and selection. Pharm Dev Technol. 2009;14:633–647.
41. Kumar M, Bishnoi RS, Shukla AK, Jain CP. Techniques for formulation of nanoemulsion systems. Int J Drug Dev Res. 2019;11:1–9.
42. Gupta A, Eral HB, Hatton TA, Doyle PS. Nanoemulsions: formation and properties. Soft Matter. 2016;12:2826–2841.
43. Tadros T, Izquierdo P, Esquena J, Solans C. Formation and stability of nanoemulsions. Adv Colloid Interface Sci. 2004;108–109:303–318.
44. Montgomery DC. Design and Analysis of Experiments. 8th ed. Wiley; 2013.
45. Danaei M, Dehghankhold M, Ataei S, et al. Impact of particle size and polydispersity index on nanoparticle characterization. Pharmaceutics. 2018;10:57.
46. Rao J, McClements DJ. Formation of flavor oil microemulsions and nanoemulsions. Food Hydrocoll. 2011;25:1413–1423.
47. Ugwoke MI, Agu RU, Verbeke N, Kinget R. Nasal mucoadhesive drug delivery. Adv Drug Deliv Rev. 2005;57:1640–1665.
48. Sinko PJ. Martin's Physical Pharmacy and Pharmaceutical Sciences. 6th ed. Lippincott Williams & Wilkins; 2011.
49. Beckett AH, Stenlake JB. Practical Pharmaceutical Chemistry. 4th ed. CBS Publishers; 2002.
50. ICH Harmonised Tripartite Guideline. Stability Testing of New Drug Substances and Products Q1A(R2). 2003.
51. Higuchi T. Mechanism of sustained-action medication. J Pharm Sci. 1963;52:1145–1149.
52. Illum L. Nasal drug delivery—possibilities, problems and solutions. J Control Release. 2003;87:187–198.
53. Andrews GP, Laverty TP, Jones DS. Mucoadhesive polymeric platforms for drug delivery. Eur J Pharm Biopharm. 2009;71:505–518.
54. Indian Pharmacopoeia Commission. Indian Pharmacopoeia. Ghaziabad: IPC; 2022.
55. Banker GS, Rhodes CT. Modern Pharmaceutics. 4th ed. Marcel Dekker; 2002.
56. ICH Harmonised Tripartite Guideline. Photostability Testing of New Drug Substances and Products Q1B. 1996.
57. ICH Harmonised Tripartite Guideline. Stability Testing of New Drug Substances and Products Q1A(R2). Geneva:

International Conference on Harmonisation; 2003.
58. Tadros T, Izquierdo P, Esquena J, Solans C. Formation and stability of nano-emulsions. Adv Colloid Interface Sci. 2004;108–109:303–318.
59. Danaei M, Dehghankhold M, Ataei S, et al. Impact of particle size and polydispersity index on the clinical applications of lipidic nanocarrier systems. Pharmaceutics. 2018;10:57.
60. Shakeel F, Ramadan W, Faisal MS. Nanoemulsions as potential vehicles for transdermal and dermal delivery of hydrophobic compounds. Saudi Pharm J. 2009;17:119–126.